Contents lists available at ScienceDirect

Chemical Engineering Research and Design

journal homepage: www.elsevier.com/locate/cherd

Enhancement of oxygen permeation fluxes of $La_{0.6}Sr_{0.4}CoO_{3-\delta}$ hollow fiber membrane *via* macrostructure modification and $(La_{0.5}Sr_{0.5})_2CoO_{4+\delta}$ decoration

Ning Han[a], *Bo Meng*[b], *Naitao Yang*[b], *Jaka Sunarso*[c,*], *Zhonghua Zhu*[d], *Shaomin Liu*[a]

[a] *Department of Chemical Engineering, Curtin University, Perth, Western Australia 6102, Australia*
[b] *School of Chemical Engineering, Shandong University of Technology, Zibo 255049, China*
[c] *Research Centre for Sustainable Technologies, Faculty of Engineering, Computing and Science, Swinburne University of Technology, Jalan Simpang Tiga, Kuching 93350, Sarawak, Malaysia*
[d] *School of Chemical Engineering, The University of Queensland, Brisbane 4072, Australia*

ARTICLE INFO

Article history:
Received 19 December 2017
Received in revised form 17 April 2018
Accepted 23 April 2018
Available online 30 April 2018

Keywords:
Decoration
Heterointerface
Hollow fiber
Membrane
Oxygen permeation

ABSTRACT

Oxygen-selective perovskite hollow fiber membrane can be used to obtain an effective oxygen separation from air at high temperature (above 700 °C) for large scale application. Here, we display that oxygen permeation fluxes of $La_{0.6}Sr_{0.4}CoO_3$ (LSC_{113}) hollow fiber membrane was enhanced by macrostructure modification and $(La,Sr)_2CoO_4$ (LSC_{214}) surface decoration. By changing the cross-section macrostructure from sandwich structure (for LSC-a fiber) to asymmetric structure (for LSC-b fiber), the oxygen flux was improved by up to 3.6-fold. Applying porous LSC_{214} decoration on LSC_{113} furthermore enhanced the oxygen fluxes for LSC-a and LSC-b, by up to 6.8-fold and 1.9-fold, respectively.

1. Introduction

Oxygen is one of the most important chemicals due to its usage in almost all major clean energy technologies, such as carbon capture and storage (Zhu et al., 2012), solid oxide fuel cells (Shao and Haile, 2004), oxidative steam reforming (Wang et al., 2016), and partial oxidation of hydrocarbons to high value-added chemicals (Othman et al., 2014). Industrial production of high purity oxygen at present however still relies on cryogenic distillation, a 100-year-old energy intensive technique (Schulz et al., 2012; Zhang et al., 2015). Therefore, a low cost and more energy efficient technique is urgently required to replace this conventional technology.

High temperature (above 700 °C) oxygen separation using dense ceramic membranes made from mixed (oxygen) ionic-electronic conducting (MIEC) materials has attracted significant interest given its advantages over the conventional cryogenic distillation, namely the absolute (100%) oxygen selectivity and the simplified operation mode (Zhang et al., 2012, 2017; Liu et al., 2013; Sunarso et al., 2008). Although this technology has matured to a small pilot plant scale stage (Tan et al., 2010a,b), its large scale application cannot manifest until MIEC materials that have both high oxygen permeability and high structure stability under operating conditions can be obtained with low cost. Among numerous MIEC materials, ABO_3-type perovskite oxides have become the focus of studies due to their high oxygen permeabilities

---

* *Corresponding author.*
E-mail addresses: jsunarso@swinburne.edu.my, barryjakasunarso@yahoo.com (J. Sunarso).

https://doi.org/10.1016/j.cherd.2018.04.038

Symbols used

E	[kJ mol^{-1}] Activation energy
J_{O2}	[mol s^{-1} cm^{-2}] Oxygen permeation flux
1/T	[K^{-1}] Inverse of temperature

Abbreviations

HRTEM	High-resolution transmission electron microscopy
LSC_{113}	$La_{0.6}Sr_{0.4}CoO_3$
LSC_{214}	$(La,Sr)_2CoO_4$
LSC-a	Hollow fiber with sandwich structure
LSC-b	Hollow fiber with asymmetric structure
MIEC	Mixed (oxygen) ionic-electronic conducting
NMP	1-methyl-2-pyrrolidinone
PESf	Polyethersulfone
SEM	Scanning electron microscopy
TEM	Transmission electron microscopy
TCD	Thermal conductivity detector
TEC	Thermal expansion coefficient
XRD	X-ray diffraction

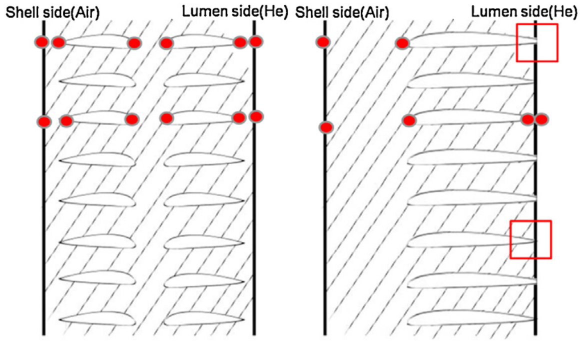

(a) Sandwich structure (b) Asymmetric structure

Fig. 1 – Schematic illustration of two hollow fibers with different cross-section macrostructures (Surface reaction sites are marked with red spots). (For interpretation of the references to color in this figure legend, the reader is referred to the web version of this article.).

and in some cases, high stabilities (Wang et al., 2015; Schlehuber et al., 2010). Ruddlesden–Popper oxides have also attracted attention because of their stable structures and their fast and anisotropic oxygen transport pathways in certain directions (Wei et al., 2011; Han et al., 2016). For oxygen separation application, these two materials have mostly been developed into disk and hollow fiber membranes (Wei et al., 2011; Han et al., 2016; Luo et al., 2011). Unlike disk membrane, which has been utilized only in laboratory studies, hollow fiber membrane is more attractive for industrial applications given its very thin transport layer and large permeation area per unit volume (Sunarso et al., 2008; Tan et al., 2010a,b). These features together with the different ends sealing options have favored the packing and utilization of hollow fibers within the membrane module (Wang et al., 2016; Han et al., 2016).

Oxygen permeation through dense MIEC membrane essentially involves two major steps, *i.e.*, oxygen bulk-diffusion (through the bulk membrane phase) and oxygen surface exchange reaction (on the feed and permeate sides), each of which can become the rate limiting step if it is the slowest step (Sunarso et al., 2008). For thick membranes, the bulk-diffusion step generally limits the oxygen permeation rate. As the membrane thickness decreases, the surface exchange reaction role becomes more dominant. In hollow fiber membrane case, the cross-section macrostructure may have major influence to its oxygen permeation rate (Zydorczak et al., 2010). Almost in all cases, however, hollow fiber membrane features sub-micron transport thickness, so that its bulk-diffusion limitation is overcome (Sunarso et al., 2008; Han et al., 2015). As a result, surface exchange reaction becomes the rate limiting step for permeation through hollow fiber (Han et al., 2016; Zhang et al., 2015). To enhance the permeation rate further, surface modification approach can be performed such as the surface roughening achievable *via* acid etching (Yang et al., 2017) or methane activation (Liu et al., 2009) and the deposition of porous metal oxide layer or active noble metal(s) or transition metal(s) on the surface (Han et al., 2015; Zhang et al., 2015; Na et al., 2017).

Sase et al. (2008) previously reported the accidental formation of perovskite oxide/Ruddlesden–Popper oxide heterophase interfaces of $La_{0.6}Sr_{0.4}CoO_3/(La,Sr)_2CoO_4$ (LSC_{113}/LSC_{214}) at the surface of 1400 °C sintered $La_{0.6}Sr_{0.4}CoO_3$ disk. Their secondary ion mass spectrometry results indicate the presence of fast oxygen incorporation paths (or the enhanced oxygen surface exchange kinetics) on the surface of these heterointerfaces (Sase et al., 2008). This phenomenon has since encouraged many more studies that reveal the potential role of dissimilar interfaces to enhance the surface oxygen exchange kinetics (Han and Yildiz, 2012). Using coherent Bragg rod analysis and density functional theory, Shao-Horn and co-workers attributed such enhanced oxygen exchange behavior to the beneficial Sr segregation at LSC_{113}/LSC_{214} interface and LSC_{214} surface due to the large driving force for Sr interdiffusion across such heterointerface (Feng et al., 2014, 2013; Gadre et al., 2012). They also reported the better retainment of the surface exchange activity with increasing annealing time on LSC_{214} deposited LSC_{113} relative to the non-deposited LSC_{113} sample. Such effect is enabled by the higher structure stability imparted by LSC_{214} so that the formation of Sr enrichment secondary particles on LSC_{113} surface is suppressed (Lee et al., 2015). It is worth noting that different from Sr enrichment, Sr segregation here is defined as Sr redistribution in the crystal lattice near the surface, accompanying the formation of secondary phases (Feng et al., 2016). Whereas Sr enrichment leads to phase instability and surface oxygen exchange degradation, Sr segregation at LSC_{113}/LSC_{214} interface elevates the O p-band center with respect to the Fermi level and enhances the surface oxygen exchange kinetics (Feng et al., 2016).

In this paper, the synthesis and characterization of two $La_{0.6}Sr_{0.4}CoO_3$ (LSC_{113}) hollow fiber membranes with distinct cross-section macrostructures are reported. The first hollow fiber exhibits sandwich structure where fingers (or macrovoids) are present on shell and lumen sides (Fig. 1(a)); denoted as LSC-a. The second hollow fiber, on the other hand, features asymmetric structure where only one finger (macrovoid) is present, which extends from the center of the fiber to the lumen side (Fig. 1(b)); denoted as LSC-b. The former has three dense layers and two isolated macrovoids sections whereas the latter has only one dense layer and one macrovoid section. These different macrostructures are anticipated to provide different oxygen permeation fluxes. It is also of interest to check the applicability of enhanced oxygen surface exchange kinetics on LSC_{113}/LSC_{214} heterointerface discussed above to oxygen permeation. To this end, the effect of depositing porous $(La,Sr)_2CoO_4$ layer on the permeate side surfaces of these two LSC_{113} hollow fiber membranes to the oxygen permeation fluxes was evaluated.

2. Experimental section

2.1. Powders and hollow fibers syntheses

$La_{0.6}Sr_{0.4}CoO_{3-\delta}$ (LSC_{113}) perovskite powder and $(La_{0.5}Sr_{0.5})_2CoO_{4+\delta}$ (LSC_{214}) Ruddlesden–Popper powders were synthesized *via* a combined citric acid-ethylene glycol complexing method, *i.e.*, Pechini sol–gel route (Tan et al., 2010a,b). Two LSC_{113} hollow fiber membrane precursors with different cross-section macrostructures were prepared using previously milled 800 °C calcined LSC_{113} powder, by varying the viscosity of the spinning mixture, *via* the combined phase inversion–sintering; the details of which are given in the